

Status of Geothermal Energy Exploration at Buranga Prospect, Uganda

James Francis Natukunda and Godfrey Bahati

Ministry of Energy and Mineral Development, Uganda. P. O. Box 9, Entebbe, Uganda

jfnatukunda@gmail.com and gbahati@gmail.com

Keywords: geology, rift tectonics, geothermometry, resistivity surveys, conceptual models

ABSTRACT

Recent studies in Buranga have used geological, geochemical, hydrogeological, and geophysical methods to elucidate the subsurface temperatures and the spatial extent of the geothermal system. The results indicate that the geothermal activity in Buranga appears to be a fault-controlled deep circulation system rather than a magmatically heated system associated with volcanoes. The geothermal surface manifestations include hot bubbling springs, water pools, gas vents (H₂S and CO₂ gas), travertine tufas, hydrothermally altered rocks and geothermal grass. Buranga has the most impressive hot springs than any other geothermal area in the Western Branch of the East African Rift System with the highest surface temperature of 98.7°C. The main geological structure is the Bwamba escarpment that forms the western part of the Rwenzori horst mountain massif. This main rift fault is cut by numerous perpendicular and oblique striking faults which together with other faults/fractures contribute to the re-charge and up-flow permeability for the geothermal fluids in Buranga. The subsurface temperatures of 120 - 150°C have been predicted by geothermometry. The results also indicate that hot springs show isotopic composition compatible with the local meteoric water line, confirming the meteoric origin of the water circulating in the geothermal system. The results from isotopes of hydrogen and oxygen ($\delta\text{D}_{\text{H}_2\text{O}}$, $\delta^{18}\text{O}_{\text{H}_2\text{O}}$) suggest that the recharge is from high ground in the Rwenzori Mountains. Micro-seismic surveys located a subsurface anomaly within the vicinity of the thermal activity in Buranga. Recently, TEM and MT surveys have been conducted in Buranga; the results and the conceptual models indicate a low resistivity anomaly underlain by a high resistivity at a shallow depth. This suggests a shallow sediment hosted outflow in addition to the fault-controlled outflow. The clayey sedimentary formations provide the cap rock of the geothermal system. Eight temperature gradient wells have been located in the prospect to test the conceptual models and discover a geothermal reservoir. The results will be used to update the conceptual models that will be a basis for locating deep exploration wells.

1. INTRODUCTION

Exploration for geothermal energy resources in Uganda has been in progress since 1930s. The studies have focused on surface exploration of three major geothermal areas: Buranga (in Bundibugyo district), Katwe (in Kasese district), Kibiro (in Hoima district) and Panyimur (in Pakwach District), all located in the Western Rift arm of the East African Rift System (EARS) (Figure 1).

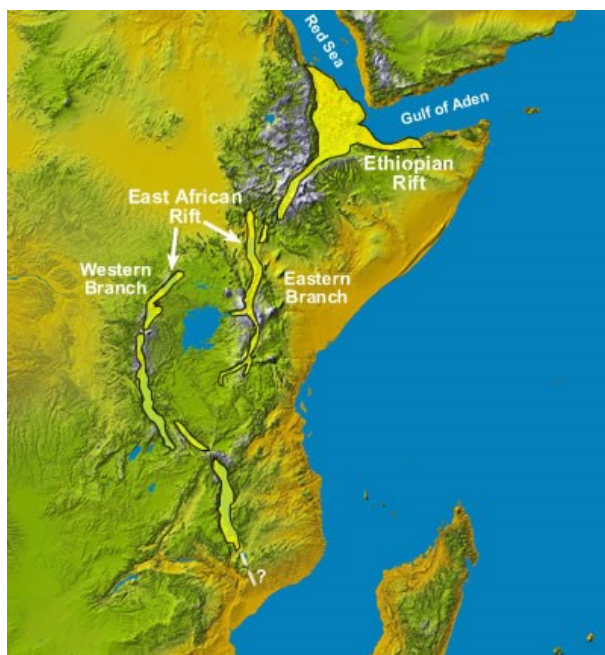
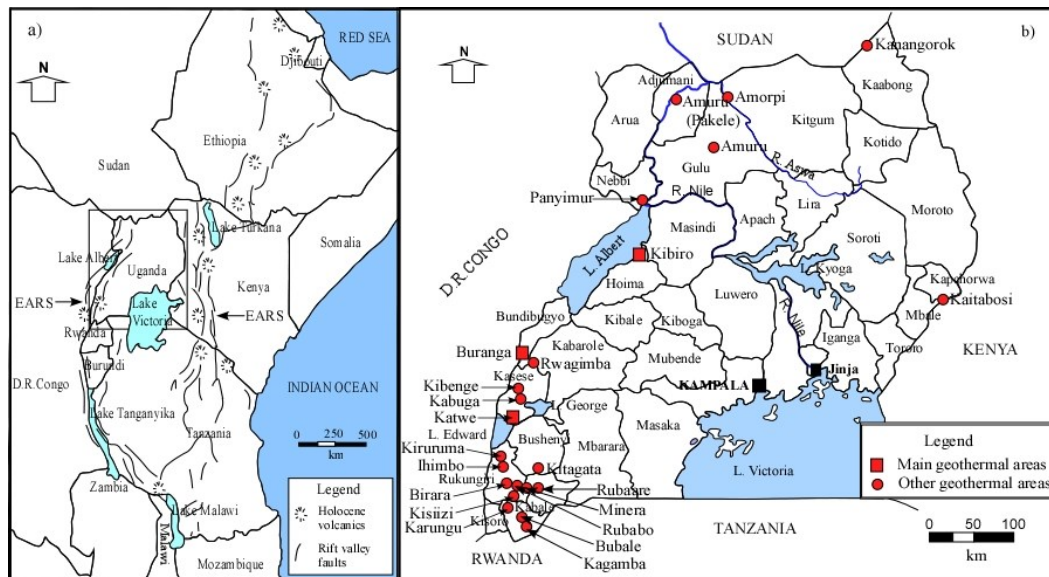


Figure 1: The East African Rift System (Source: James Wood and Alex Guth; the base map is a Space Shuttle radar topography image by NASA).

The Albertine Rift forms the northern part of the western arm of the EARS. The East African Rift is an active continental rift zone that appears to be a developing divergent tectonic plate boundary in East Africa. The rift is a narrow zone in which the African Plate is in the process of splitting into two new tectonic plates, known as the Somali Plate and the Nubian (or African) Plate, all of which are sub-plates or protoplates (Wood and Guth, 2014).



2. LOCATION OF BURANGA GEOTHERMAL PROSPECT

3. GEOLOGY

The geology of Uganda consists of an exposed pre-Cambrian basement dissected by the western branch of the EARS in the western part of the country (Figures 1 and 2). The eastern branch, the Gregory Rift, passes through the central part of Kenya and Tanzania. The Western branch, (part of which in Uganda is referred to as the Albertine Rift), starts to the north along the Sudan border, and then curves to the west and then southwest along the border with the DRC, and south to Rwanda, Burundi and western Tanzania. Spreading began at least 15 million years ago in Miocene time. The western Rift is considered to be at an early stage in the development and is younger (late Miocene-Recent) than the more mature eastern branch (Morley and Westcott, 1999). The Albertine rift is seismically active, characterized by deep-seated (15-30 Km) large earthquakes (Tugume, 2010). The region of the Rift has a markedly higher heat flow than the surrounding Pre-Cambrian terrain. Two different echelon strands are found in the Western Rift Valley, separated by the Rwenzori Mountains, which rise from a base of less than 1,000 m in the Rift to over 5,000 m elevation. Within the Rift Valley there are thick layers of late Tertiary and Quaternary sediments, fresh water and saline crater lakes, volcanic, and plutonic bodies have been identified beneath L. Albert and L. Edward (EDICON, 1984).

Buranga hot springs are located at the north-western foot of the Rwenzori massif near the base of Bwamba escarpment and localized by major Rift Valley faults (Figure 3). The hot springs emerge through sediments of Kaiso beds and peneplain gravels that consists of variable sands and gravels with irregularly distributed sub-angular boulders. The Kaiso sediments are underlain by fine to medium-grained, poorly consolidated sands and clays (some coated with calcareous material) and occasional tuffs.

Geophysical surveys confirmed the presence of these sediments down to a depth of 1,524 m. The boreholes drilled in 1950s showed that the Tertiary succession was terminated in the fault zone by a breccia cemented by calc-tuffs followed by mylonite (Harris et al., 1956). The clays are of various colours and the sands are fine-to medium-grained, varying in colour between white, brown, grey and green. The most common binding material is clay, although this may be patchily replaced by calcium carbonate, giving rise to calcareous sandstones and grits. Pebble beds are of rare occurrence and there are no fossils present apart from plant fragments. Close to the Buranga hot springs, a fault line (striking between 20° and 45° and dipping 60-65° westwards) is exposed (Johnson and McConnell, 1951). The mylonite rocks characterize the fault zone suggesting movement along a very old fracture zone of compression. Further north, the fault system displays both a change of direction and dip reduction. The topographic features indicate

that step faulting is also present (Harris et al., 1956). Precambrian rocks of the main rift fault, which strikes N45°E and dips N60-65°E, underlie the sediments.

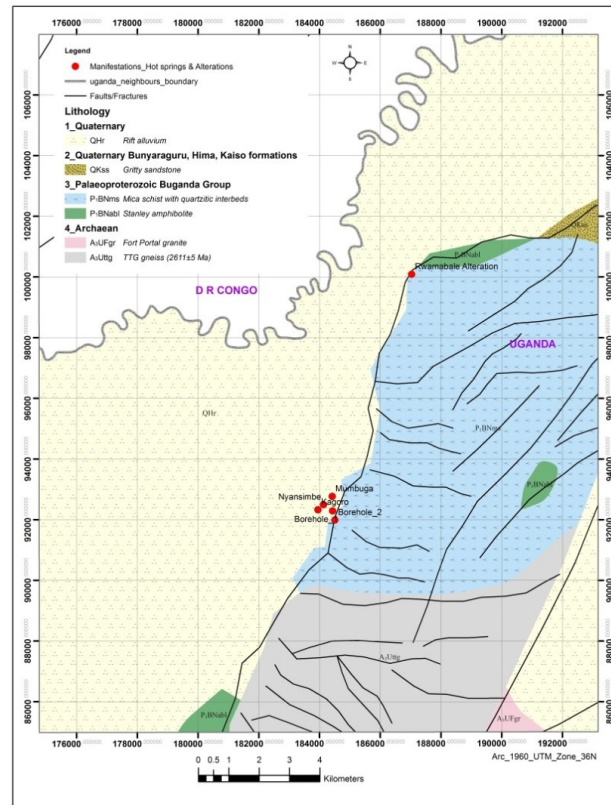


Figure 3: Geology of Buranga area. (GIDS Consult Ltd, 2016.)

The rocks around the northern half of Rwenzori massif in which Buranga is located consist mainly of migmatites, gneisses and amphibolites. There are four lithological units which fall in Archaean, Palaeoproterozoic Buganda Group and Quaternary ages. The Archaean is represented by the TTG gneiss in the south and Fortportal granite in the northeast. The Palaeoproterozoic Buganda Group is represented by the Stanley amphibolite and the mica schist rock that is intruded by quartzitic inter-beds (Figure 3).

The *TTG gneiss* (2611 ± 5 Ma) (*A3Utg*) consists of rocks with variable granitoid compositions namely, granites, granodiorites, and tonalites to trondhjemitic (Westerhof et al., 2012). U-Pb age determinations of zircon cores (Laser-ICP-MS method) from the foothills gneisses of the Rwenzori Mountains yielded the following ages: 2584 ± 18 Ma, 2637 ± 16 Ma and 2611 ± 14 Ma (Link et al. 2010). The *Stanley amphibolite* (*P1BNabl*) is hornblende-rich, garnet-bearing amphibolites in which medium-grained, foliated rocks have coarse amphibole segregations and epidote and quartz veins. The sequence begins with quartzites, which unconformably overlie Archaean gneisses. Quartzites show festoon crossbedding and ripple marks. The upper unit is phyllitic schist with sedimentary structures. Tholeiitic Stanley metavolcanics occur as interlayers in these schists. They are characterised by pillow lava structures, which demonstrate a volcanic origin for these fine-grained amphibolites and tuffaceous volcanoclastics. The *Mica schist with quartzitic interbeds* (*P1BNms*) has a gneissose appearance and partly garnet bearing. Pegmatitic dykes intrude these rocks in several places. Generally, the lithological units strike N10-30°E and have complex joint systems. The hot springs seem to lie on a fracture/fault line striking N40°E parallel to main rift fault (Gislason et. al., 1994).

4. GEOTHERMAL MANIFESTATIONS OF BURANGA PROSPECT

Buranga has the most impressive surface geothermal manifestations with a wide areal coverage in the whole of the Western Branch of the East African Rift System. The geothermal manifestations are found at the foot of the escarpments in a swampy area enclosed by a dense rain forest. The geothermal surface manifestations are localised in three areas namely Mumbuga, Nyansimbe and Kagoro (Figures 3, 4, 5). At Mumbuga, the eruptive hot spring, bubbling hot springs, hot grounds, solfatara occur.

At Nyansimbe, a large steaming water pool with several springs and travertine occur (Figure 4).



Figure 4: Erupting hot spring at Mumbuga area. Note the calcareous tufa cone building up from the spring waters (Photo taken by Natukunda in 2016).



Figure 5: Nyansimbe water pool with several hot springs and travertine around it (Photo taken by Natukunda in 2016).

At Kagoro, travertine cones, hot springs, sulphurous deposits occur (Fig. 6).



Figure 6; Kagoro travertine tufa cone (Photo taken by Natukunda in 2016).

The three manifestation areas at Buranga are characterized by H_2S and geothermal grass that covers large swampy parts of manifestation areas. The surface temperature is $98.7^{\circ}C$ and the flow is approximately 10-15 litres/second, an indication of high permeability.

5. GEOTHERMAL MAPPING

Detailed mapping of the geothermal surface manifestations has been done at Buranga geothermal prospect. Seventy-six of the hot springs ($> 31^{\circ}C$) at Buranga were mapped with GPS in September 2017 (Figures 7 and 8). Mapping included temperature probe measurements at up to 1 m depths in the pools to find the hottest inflow points, noting the distribution of active and inactive travertine deposition, and noting local alignments of springs along probable fissures. In addition to acquiring temperatures of hot springs, an additional 22 soil temperature measurements were obtained between the hot springs to help distinguish background temperatures relative to the thermal areas. This included a half dozen soil and spring temperature measurements were also made along an E-W transect about 500 m north of the hot springs and all temperature measurements in that area were within background temperatures ($22-24^{\circ}C$) (EAGER, 2017, U23 – D02).



Figure 7: Recording temperature of a hot spring along the forest/grassland interface near drill hole exploration number 3 (EAGER, 2017, U23 – D02).

The distribution of hot springs covers a triangular shaped area 0.5 km wide east-west, and 0.5 km wide north-south, for a total area of 0.125 km² (Fig. 8). This area covers nearly the entire area that is visibly devoid of trees southeast of the line of named hot springs. Hot spring pools range from 10 cm to several meters across, with most of them < 1 meter across. Pool depths range from a few cm to a couple meters.

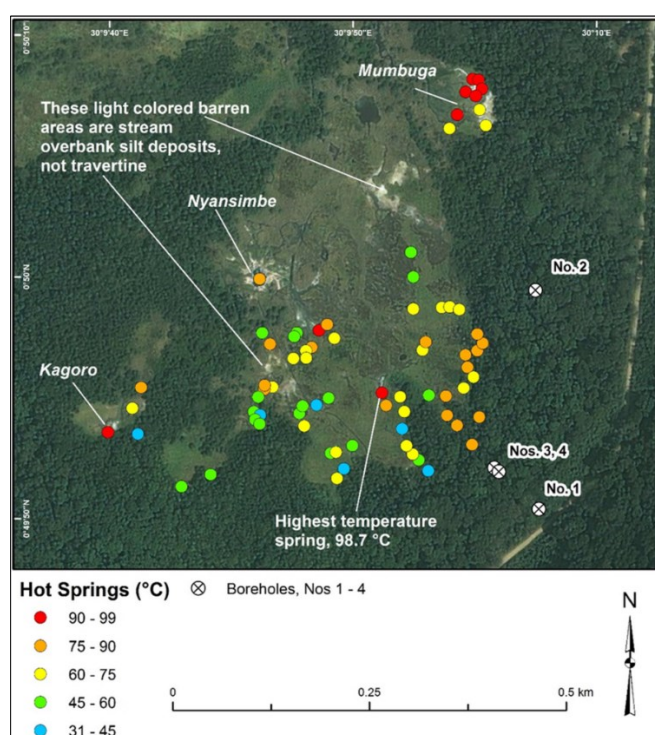


Figure 8: Map of active hot springs and existing drill holes at Buranga. (EAGER, 2017, U23 – D02).

Of the 76 hot springs measured in this area, four separate clusters of hot springs measured > 90°C. These include the cluster of hot springs at Mumbuga, Kagoro and two other unnamed hot springs southeast of Nyansimbe, including the hottest spring at Buranga which is boiling vigorously at 98.7°C (temperature for boiling at about 670 m elevation above sea level). The cluster of hot springs at Mumbuga includes six separate springs >92°C, and a maximum temperature of 93.5°C. The maximum measured temperature at Kagoro was 91.3°C. Three areas in the hot spring field had closely spaced, cm- to dm- to m-spaced hot springs tightly aligned over 10-20 m distance; these may represent spring fissures along faults or fractures in the basin-fill deposits. These spring alignments along possible fissures are all oriented about N20°E, which is sub-parallel to local range-front fault. These fissures were at Kagoro, Mumbuga, and at the unnamed 98.7°C spring (Fig. 9) in the southeast-central part of the Buranga hot springs field (EAGER, 2017, U23 – D02).



Figure 9: Looking SSW at an alignment of closely spaced hot springs along a N20°E trending fissure (EAGER, 2017, U23 – D02).

6. STRUCTURAL FRAMEWORK

The range-front fault system in the vicinity of the Buranga geothermal area makes several 0.5 to 1 km left and right steps (Fig. 10). Locally, the Buranga geothermal area sits adjacent to a 0.5 km wide, left step along the range front. Additionally, a NE-striking, northwest-dipping fault intersects the range-front fault directly north of the hot springs area. Five fault surface measurements were mapped along the primary range-front fault trace (Bwamba Fault) adjacent to the Buranga geothermal area. The average strike orientation of these fault surface measurements was N23°E and had dips ranging from 50° to 60° W. The average dip for these five measurements on this segment of the range-front fault is 55° W. Overall, these dip measurements were not greatly different than the approximation of 64° that was based off a trigonometric calculation using the depth of the fault intersected by drill hole 1, and the horizontal distance to the perceived fault trace along the range-front. Crude striations were observed locally on the fault surface with near 90° rake. These indicate pure dip-slip motion along this segment of the range-front fault, and which is consistent with regional WNW-ESE oriented extension recognized across this part of the Albertine Rift (EAGER, 2017, U23 – D02).

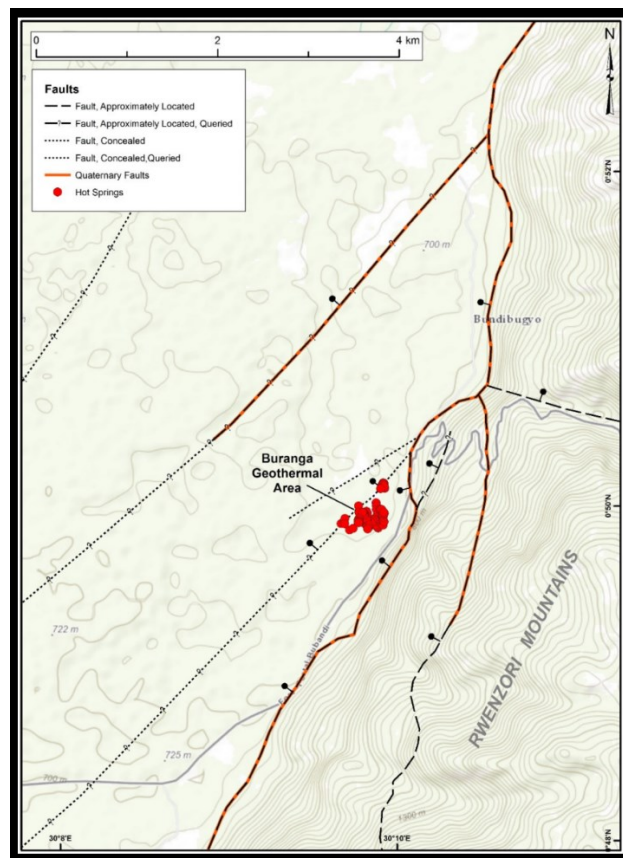


Figure 10: Structural geology of Buranga geothermal field area (EAGER, 2017, U23 – D02).

The Buranga geothermal area sits along a 0.5 km-wide step in the range-front fault along the northwest side of the Rwenzori Mountains (Fig. 10). This step is also coincident with an intersection with an inter-basinal fault, synthetic to the main range-front

fault. The local and regional geotechnical data indicate that these faults are nearly pure dip-slip, making this setting a step-over between pure normal faults in contrast to a pull-apart between oblique- or strike-slip faults (EAGER, 2017, U23 – D02).

At Buranga, the hot springs about a concealed NE-striking fault along the NW side of the hot springs field (Fig. 10). Hot springs have not been identified NW of this concealed fault. Thus, it is possible that this Fault may be a barrier, or both a barrier and a conductor of fluid flow. South of this concealed, NE-striking fault, several hot spring fissures were observed with approximate N20°E trends (Fig. 10). Furthermore, at map scale, several higher temperature spring clusters (e.g., > 70°C) are also aligned along N to NNE trends. These N to NNE trends of hot springs are parallel to the local range-front fault and may indicate that a number of N- to NNE-striking faults and fractures underline the hot springs field between the range-front fault and the outer, NE-striking concealed normal fault (Fig. 9) (EAGER, 2017, U23 – D02).

7. GEOCHEMISTRY

7.1 Hydrochemistry

The concentrations of Cl^- , SO_4^{2-} and HCO_3^- in Buranga geothermal waters are similar and therefore indicators must be used with caution, and the high Cl relative to Li and B concentrations suggest relatively old hydrothermal a system (Giggenbach, 1991). The results of analysis of volatiles and physical parameters, and major constituents are presented in Tables 1 and 2 respectively.

Table 1: Results of analysis of volatiles and physical parameters. Concentrations in mg/kg.

Location	Sample no.	Temp. (°C)	pH	EC (µs/m)	CO ₂	H ₂ S	SiO ₂	TDS
Mumbuga	BR-11-001	93.6	7.73	19550	2411	<0.05	76.0	14000
Nyansimbe-Pool	BR-11-002	85.8	7.81	21650	2878	<0.05	85.8	17050
Kagoro	BR-11-003	89.0	7.50	21600	2798	0.06	81.0	16400
Mungera Stream	BR-11-004	21.8	7.52	169.8	57	<0.05	36.9	74

The fluids are neutral with a pH of 7-8 and salinity of 14,000 – 17,000 mg/kg total dissolved solids. Plausible solute geothermometers tested for several hot springs and pools predict a subsurface temperature was 120 - 150°C for the Buranga prospect. The gas composition is dominated by CO₂ and has no H₂ which suggests that the subsurface temperature is less than 200°C (Ármannsson, 1994).

Table 2: Analytical results of major constituents. Concentration in mg/kg.

Sample No.	Na	K	Ca	Mg	SO ₄	Cl	F	Fe	Al	B	Sr	Li	Br
BR-11-001	5160	190	2.56	2.27	3570	3490	27.2	0.05	0.014	4.2	2.46	1.3	16.4
BR-11-002	6300	234	2.04	1.98	4420	4240	31.5	0.01	0.017	4.8	2.15	1.54	20.4
BR-11-003	5950	219	2.69	2.19	4160	4030	30.8	0.02	0.019	4.7	2.54	1.47	19.6
BR-11-004	11.1	3.7	11.2	3.61	1.7	1.8	0.17	0.02	0.011	0	0.08	0.01	0

7.2 Isotope hydrology

The δD and $\delta^{18}\text{O}$ data all plot close to the line with equation $\delta\text{D} = 8 \cdot \delta^{18}\text{O} + 12.3$, the Local Meteoric Water Line (LMWL), obtained from rainwater samples from Entebbe (GNIP, 1999). There are no signs of oxygen shift from this line so that reasonable permeability is inferred as is expected from the physical characteristics of the geothermal system. The isotope composition of the geothermal water is depleted in both δD and $\delta^{18}\text{O}$ compared to the local cold ground- and river waters suggesting that the geothermal water is from high ground in the Rwenzori Mountains (Fig. 11). A subsurface temperature of 200°C is predicted by isotopic geothermometers. There is no tritium in the thermal water from Buranga which implies that it is not a mixture of hot water and cold groundwater. The strontium ratios in rocks indicate that the geothermal water, most likely, interacts with granitic gneisses. The source of sulphate is minerals or rock (terrestrial evaporates) with a possible magmatic contribution (Bahati et. al., 2005). Studies by the Federal Institute for Geosciences and Natural Resources (BGR) of Germany and the Government of Uganda using helium isotopic ratio ($^3\text{He}/^4\text{He}$) in gaseous discharges from hot springs also suggest a magmatic source of solutes for Buranga (BGR-MEMD, 2007).

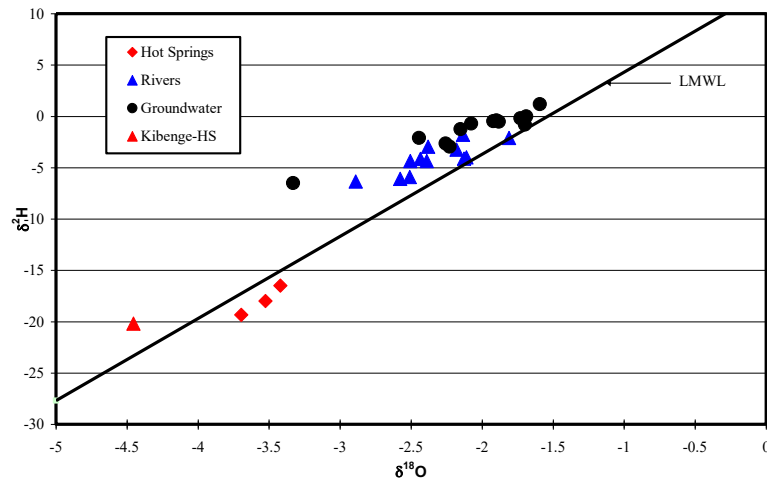


Figure 11: Buranga. Stable isotopic composition of hot and cold water samples (reference).

8. GEOPHYSICAL INVESTIGATIONS

8.1 Micro seismic surveys

BGR-MEMD carried out micro-seismic surveys at Buranga and surroundings. The distribution of earthquakes recorded within the year 2007 is presented in Figure 12. The concentration of earthquakes around Buranga hot springs suggests an area of weakness around the hot springs. This may indicate a tectonically active fracture or fault zone for Buranga Ochmann (2007).

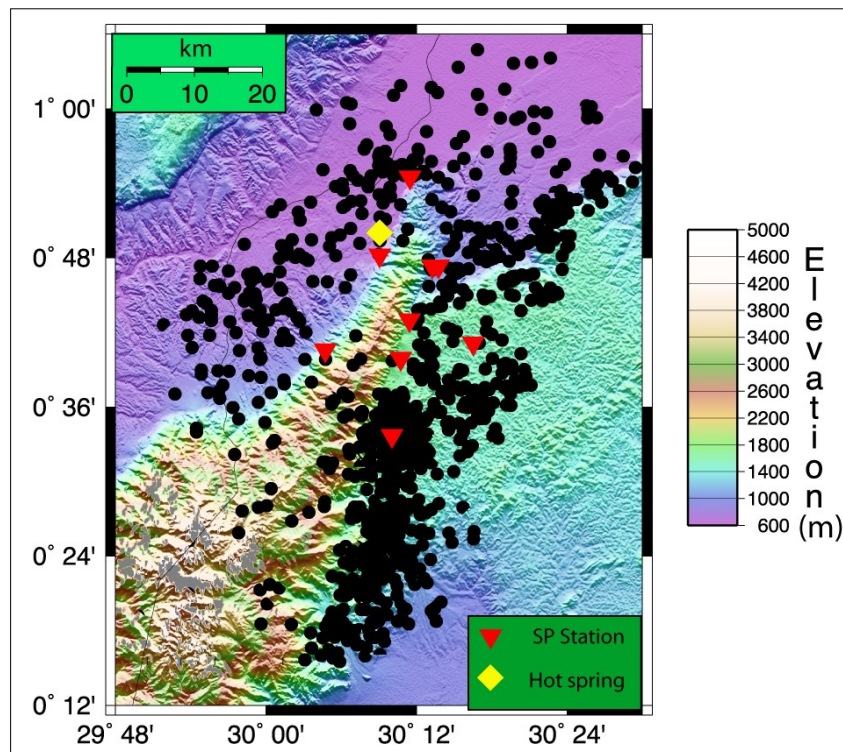


Figure 12: Distribution of earthquakes in Buranga and surroundings (sources: BGR-MEMD, 2007).

8.2 MT and TEM surveys

The two techniques used were Transient Electro-magnetic (TEM) and Magneto-tellurics (MT) surveys. The TEM survey was aimed at mapping shallow structures and for static shift correction on the MT soundings made on the same site, and the MT survey was used to map deeper resistivity structures of the area. During the three surveys campaigns carried out in 2015, 2016 and 2017, 133 pairs of MT and TEM soundings were made in the Buranga prospect covering area of 120 Km² (Figure 13).

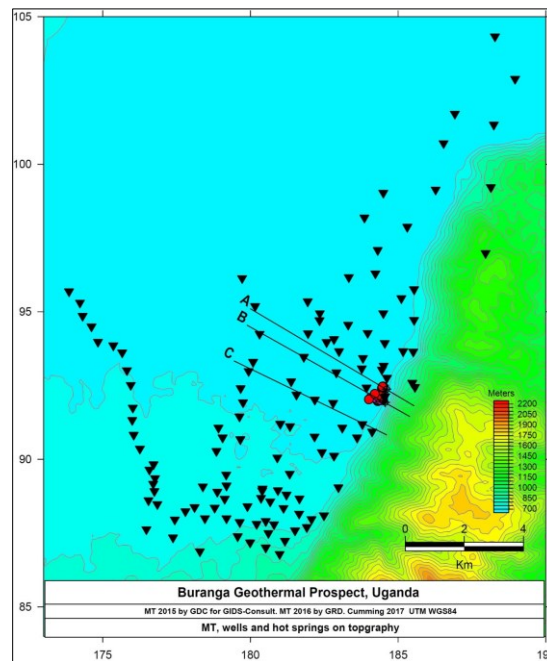


Figure 13: Location of the survey point for MT and TEM soundings.

9. CONCEPTUAL MODELS OF BURANGA PROSPECT

The Buranga geothermal system is likely to be in a temperature range of 110°C - 150°C. The heat source for the Buranga springs is likely to be deep circulation in Precambrian crystalline rocks near the margin of the graben; isotopic models indicate recharge the adjacent Precambrian highland (Mt Rwenzori ranges). A local recharge rather than an extensive lateral diversion in sediments is also indicated by the high flux of gas with composition indicating a deep crustal origin. The high salinity and sulphate of the springs and their overall chemistry strongly suggests that, before significant dilution occurs, the hydrothermal system encounters evaporites like the gypsum.

Because of the prolific nature of the springs and the indications of mainly deep flow in the Precambrian but with significant modification in the sediments, one conceptual model includes a sedimentary aquifer that intercepts the deep up flow hosted in a structural intersection zone. A prolific shallow sedimentary outflow aquifer might be a viable target that would be lower cost to explore and drill than a deeper fault-hosted system.

The conceptual models proposed for Buranga include: 1) down-flow from the highland to the east and up flow in fault/fracture hosted permeability within the damage zone and fault splays directly associated with the Hot Springs Fault trace; 2) down-flow within the basin and up flow within the damage zone and fault splays directly associated with the Hot Springs Fault trace; 3) either scenarios 1 or 2 coupled to up-dip outflow in a sand or gravel formation westward toward the basin, and 4) 1 or 2 and maybe 3 coupled with a very shallow outflow from the hot spring fault to the basin margin to the east (EAGER, 2017, U23 – D03).

Figures 14 and 15 show median conceptual model along Profiles A and B. the models indicate a 125°C up flow in a damage zone adjacent to the Hot Springs Fault that outflows a few 100 m into shallow sediments near the hot springs. The dip of the main fault is 55° based on surface structure mapping, not the MT.

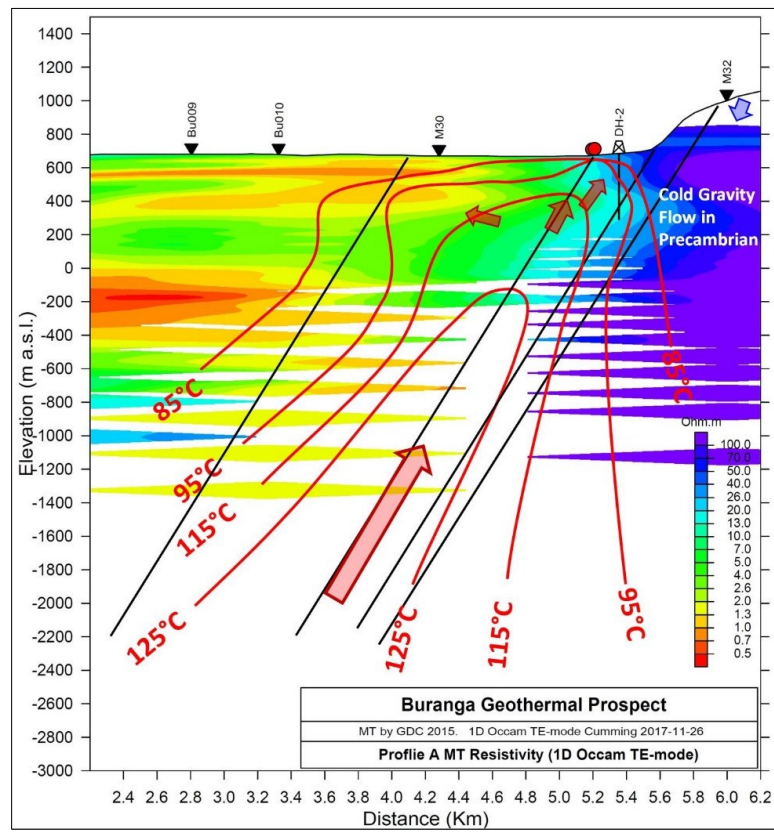


Figure 14: Median conceptual model of Buranga geothermal prospect along Profile A (EAGER, 2017, U23 – D03).

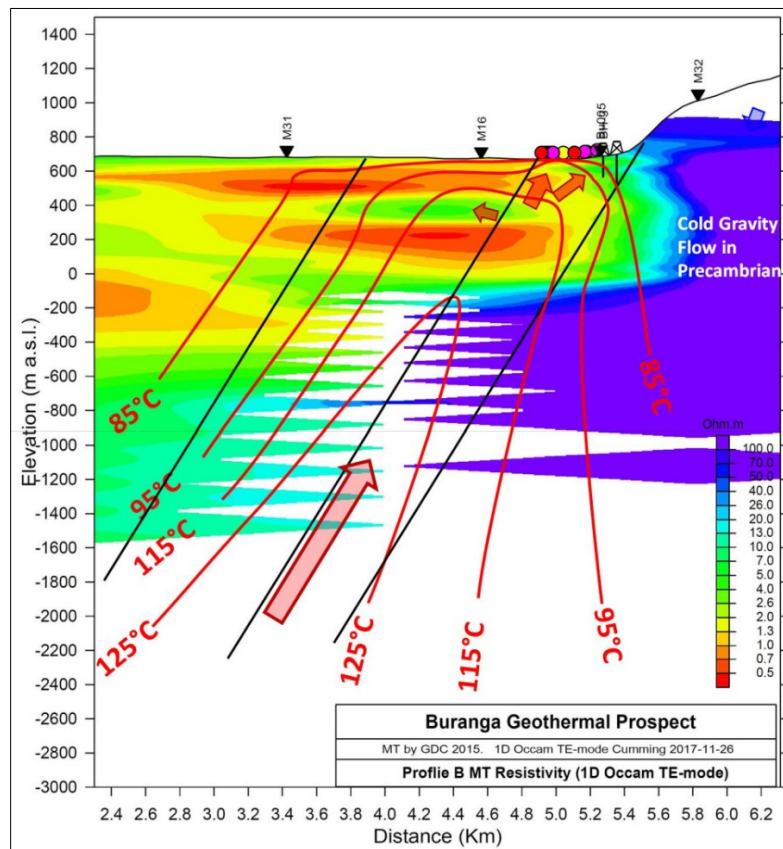


Figure 15: Median conceptual model of Buranga geothermal prospect along Profile B (EAGER, 2017, U23 – D03).

Figure 16 illustrates a variation on the model in Profile B that includes an optimistic wide up flow that carries 125°C to <500 m depth. Although omitted from this figure, a 150°C contour is implied by the model.

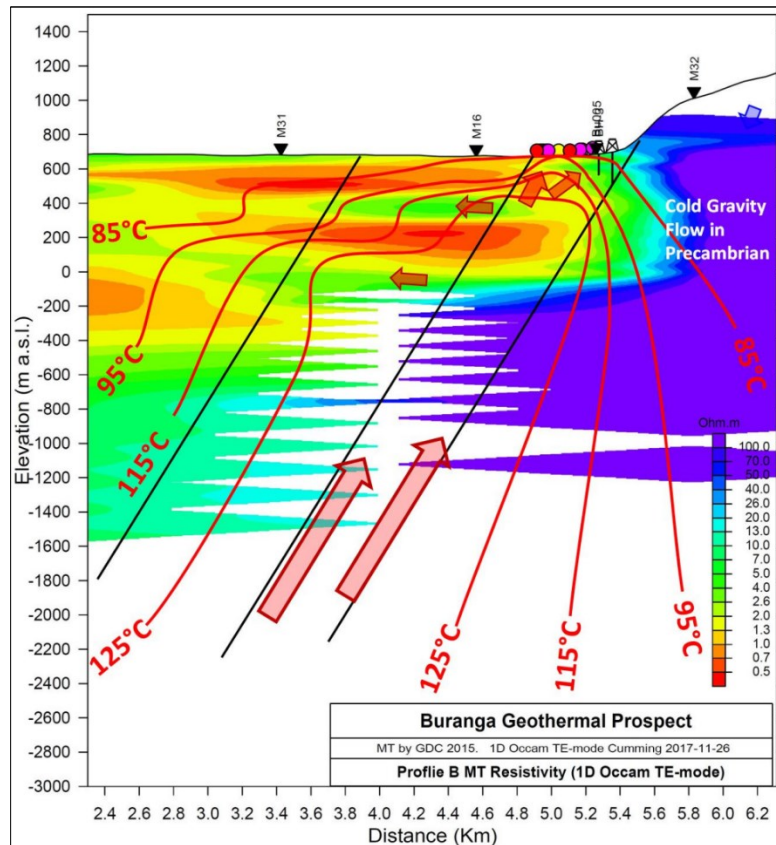


Figure 16: Buranga optimistic conceptual model along Profile B (EAGER, 2017, U23 – D03).

6. CONCLUSIONS

Buranga has impressive geothermal surface manifestations; Buranga springs have the highest surface temperatures (98.7°C), highest surface heat flow and highest hot water flow than all other explored geothermal prospects in Uganda. Subsurface temperatures of 110-150°C are inferred by geothermometry in Buranga. These temperatures, if confirmed, are good for electricity production and for direct use in industry and agriculture. Isotope hydrology results indicate the source of the geothermal fluids in Buranga to be from high ground in the Rwenzori Mountains whose faulted and fractured nature provides adequate permeability necessary for recharge and thermal fluids in Buranga.

The geochemistry of the three sets of Buranga hot springs, their geological setting and geophysical constraints are consistent with a 110 to 150°C geothermal resource heated by a fault-hosted, deep-circulation (non-magmatic) up flow system with some potential for a shallow sediment-hosted outflow analogous some of the geothermal systems in the Basin and range region systems like Don Campbell in Nevada, USA. The heat flow from the prolific springs in Buranga and the geothermometry from 110 to 150°C lead to a higher likelihood of resource existence and higher estimates of capacity for a resource at Buranga than other prospects in Uganda.

7. RECOMMENDATIONS

- Conduct TEM/MT surveys (300-500m inter-station spacing) around the hot spring area to delineate the boundaries of the geothermal reservoir and delineate the heat source.
- Observe temperature gradient wells to follow up geophysical surveys that is more focused on the hot spring area because of the likely deep origin of the geothermal system and the ambiguity in the interpretation of the shallow sediment-hosted resource.
- Update geothermal models and locating of deep exploration drill sites; drilling at 2-3 exploration wells in the delineated geothermal anomalies and location of production wells.
- Carry out environmental and social impact assessment for geothermal power production and direct uses.
- Install well-head power plants for electricity production.
- Study direct use applications of the Buranga geothermal fluids like fishing industry along River Semuliki, drying of coconuts (a chief cash crop in the area), preservation/ pasteurization of milk and tourism (spa).

REFERENCES

- Ármannsson, H., 1994. "Geochemical Studies on three geothermal areas in West and Southwest, Uganda". Final Report. Geothermal Exploration UGA/92/003, UNDES, GSMD, Uganda, 85pp.
- Bahati, G., Z. Pang, H. Ármannsson, E.M. Isabirye, V. Kato, 2005. "Hydrology and reservoir characteristics of three geothermal systems in Western Uganda", *Geothermics*, 34, p.568-591.
- BGR-MEMD, 2007. "Detailed surface analysis of the Buranga geothermal prospect, West-Uganda". Final terminal report, 168 pp.
- EAGER, 2017; "Structural Geology at Panyimur and Buranga". Report U23 – D02.
- EAGER, 2017; "Enhanced resource modeling for Panyimur and Buranga" Report U23 – D03.
- EDICON, 1984: "Aeromagnetic interpretation of Lake Albert/Edward portion of the Western Rift Valley". Unpubl. report, EDICON inc., Denver Colorado, sept. 1984.
- GIDS Consult Ltd, 2013. "Reconnaissance Geothermal Investigations of Exploration Area (EL) 275 and its surroundings". GIDS Consult Ltd., Progress Report 1, 2013.
- GIDS Consult Ltd, 2016. "Report of work done on EI0725" – Buranga. Unpublished report Directorate of Geological Survey and Mines, Uganda.
- Gigenbach 1991. "Applications of geochemistry in geothermal reservoir development".
- Gislason, G., G. Ngobi, E.M. Isabirye, and S. Tumwebaze, 1994. "An Inventory of three Geothermal Areas on West and Southwest Uganda". Prepared by the United Nations for a Project of the UNDP.
- GNIP, 1999: "Data from the Global Network for Isotopes in Precipitation (GNIP) since 1960". Site Entebbe (Airport), Uganda; latitude 0°05'0" N and Longitude 32°45'0" E.
- Harris, N., J.W. Pallister and J.M. Brown, 1956: "Oil in Uganda". Memoir No. IX, Geological Survey of Uganda, 33 p.
- James Wood and Alex Guth. "East Africa's Great Rift Valley: A Complex Rift System. Michigan Technological University", <http://geology.com/articles/east-africa-rift.shtml> (Tuesday 28 May 2014).
- Link, K., Kohn, D., Barth, M., Tiberindwa, J., Barifaijo, E., Aanyu, K. & Foley, S. 2010. "Continuous cratonic crust between the Congo and Tanzania blocks in western Uganda". *International Journal of Earth Sciences / Geol. Rundschau* 99 (7), 1559 – 1573.
- McNitt, J.R., 1982. The geothermal potential of East Africa. In *Proceedings of the Regional Seminar on Geothermal Energy in Eastern and Southern Africa*, Nairobi, Kenya. P. 3 - 8.
- Morley, C. K., D. K. Ngenoh, and J. K. Ego, 1999a: "Introduction to the East African Rift System, in C. K. Morley ed., *Geoscience of Rift Systems – Evolution of East Africa*: AAPG Studies in Geology No. 44, p. 1 – 18
- Ochmann N, Lindenfeld N, Barbirye P and Stadtler C, 2012. "Microearthquake survey at the Buranga geothermal prospect, western Uganda".
- PEPD, 2008. "Petroleum Potential of the Albertine Graben, Uganda, November Brochure, 2008. Petroleum Exploration and Production Department, Entebbe, Uganda".
- Tugume, 2010. "The Depth Distribution of seismicity at the northern Rwenzori Mountains: Implications for heat flow in the Western rift, Uganda".
- Wayland, E.J., 1935. "Notes on thermal and mineral springs in Uganda". *UGSM Bull.* 2, p. 44-5.
- Westerhof et al 2012. "Geology and Geodynamic Development of Uganda with Explanation of the 1:1,000,000 Scale Geological Map". 406 pp.